Pergamon

PII: S0022-3697(98)00047-X

J. Phys. Chem Solids Vol 59, No. 8, pp. 1241–1249, 1998
0022–3697/98/$ – see front matter

ORIGIN OF THE BLUE LUMINESCENCE OF β-Ga_2O_3

LAURENT BINET and DIDIER GOURIER

Laboratoire de Chimie Appliquée de l'Etat Solide, URA CNRS 7574, Ecole Nationale Supérieure de Chimie de Paris, 11 rue Pierre et Marie Curie, F-75231 Paris cedex 05, France

(*Received* 6 *June* 1997; *accepted* 11 *March* 1998)

Abstract—Electrons in donor states of gallium oxide exhibit a paradoxical behavior. On the one hand they exhibit free electron properties such as impurity band conduction and motionally narrowed ESR signals at liquid helium temperature, while on the other hand they are responsible for a blue luminescence characterized by a strong electron–phonon coupling. The time decay and the temperature dependence of the blue luminescence upon specific excitation of the acceptor defects were investigated and a model for the donor V_O^X and acceptor $(V_O, V_{Ga})'$ microstructure is proposed. Donors would be assembled in shallow clusters responsible for delocalized electron behavior with minority acceptors between. The blue luminescence would result from the fast recombination of an exciton trapped at an acceptor site after a rate determining tunnel capture of an electron from a donor cluster.

Keywords: A. oxides, D. defects, D. luminescence, D. electron paramagnetic resonance (EPR), D. electrical conductivity

1. INTRODUCTION

Gallium oxide, β-Ga_2O_3, is a wide band gap compound ($E_g \approx 4.9$ eV) [1] which has long been known to exhibit both conduction [2–4] and luminescence properties [5–8]. When prepared under reducing conditions, gallium oxide becomes an *n*-type semiconductor, due to oxygen vacancies, which act as shallow donors with ionization energy $E_d \approx 0.03$–0.04 eV [2]. The structure of β-Ga_2O_3 is monoclinic with space group C2/m and contains both octahedral and tetrahedral cation sites in equal quantities and arranged in parallel chains along the *b* axis. It was shown by semi-empirical band structure calculations that the top of the valence band is formed by non-bonding 2*p* oxygen orbitals, while the bottom of the conduction band is predominantly constituted of 4*s* octahedral gallium orbitals, with no contribution of AOs from the tetrahedral gallium ions, which lie at higher energy [9]. This band structure turned out to be in good agreement with earlier observations [10] on optical absorption in gallates, which showed that the absorption edge in gallates with octahedrally coordinated Ga^{3+} lies at lower energy than in compounds with tetrahedrally coordinated Ga^{3+}.

More recently, a renewed interest in β-Ga_2O_3 has arisen since β-Ga_2O_3 is a transparent conducting oxide and has potential applications in optoelectronic devices [11]. Also, the magnetism of the conduction electron spins in this material exhibits an original memory effect within a wide range of temperature from 4 K to at least room temperature [12]. This effect manifests itself as a bistable magnetic resonance of conduction electron spins due to a bistable dynamic nuclear polarization of gallium nuclei by conduction electrons. This phenomenon is so far the most easily observable memory effect in a two-level quantum system. Great efforts were made to understand the relationship between this new property and the material structure [13] and presently particular attention is paid to the influence of the donor microstructure upon bistable conduction electron spin resonance (BCESR). Since the conduction electrons at the origin of BCESR come from oxygen vacancies and that these defects are also known to be correlated to a strong blue luminescence [6, 8], the investigation of the optical properties of β-Ga_2O_3 can provide valuable information about the donor microstructure.

Many observations on the luminescence of gallium oxide have been reported in the literature, which can be summarized as follows. Upon optical excitation through the band gap, β-Ga_2O_3 can exhibit up to three different emissions, UV, blue and green, according to the sample preparation and the nature of the dopant [5–8]. Only the UV emission is independent of the sample history and was attributed to the recombination of a self-trapped exciton [14, 15]. The green emission occurs only in the presence of specific impurities such as Be, Ge and Sn but its mechanism is still not thoroughly clarified [6, 8]. The blue luminescence is produced only in conducting samples, either as-grown or doped with Zr^{4+} or Si^{4+} [6, 8], which demonstrates that it is related to the presence of oxygen vacancies. The blue emission can also be selectively excited at liquid helium temperature with photon energies slightly smaller than the band gap, indicating that it originates from the excitation of defects

in the forbidden gap [8]. It has been suggested that this blue emission could be produced by a tunnel recombination of an electron on a donor V_O^x with a hole on an acceptor which could be either V_{Ga}''' [8] or a pair of charged vacancies $(V_O, V_{Ga})'$ [16]. Another important point is that both UV and blue emissions are broad and exhibit important Stokes shifts, characteristic of a strong electron–phonon coupling, which means that the recombining electrons and holes are localized [6–8].

These characteristics of the luminescence in β-Ga_2O_3 are apparently in contradiction with our observations on the ESR properties of gallium oxide, which provide evidence of electron delocalization [12]. As a matter of fact, although some ESR experiments on β-Ga_2O_3 reported in the literature do not mention any conduction electron spin resonance (CESR) signal [7, 17], our samples do exhibit a motionally narrowed CESR signal from 4 to 300 K [12]. The dynamic nuclear polarization observed at all temperatures in the range 4–300 K is also strong evidence of delocalized electrons. The existence of these properties at liquid helium temperature shows that with donor concentrations $N_d \approx 10^{18}$–10^{19} cm^{-3} usually obtained in Ga_2O_3 [2, 12], the Mott criterion [18] is achieved, so that the donor orbitals form an impurity band. Therefore in our samples the electrons, even in donor states, are delocalized and exhibit a degenerate semiconductor behavior.

In this paper we first show that samples with delocalized donor states exhibit the same luminescence properties as those reported in the literature. Then investigation of the temperature and time dependence of the blue luminescence upon specific excitation of the acceptor defects will allow us to suggest a model that reconciles both the delocalized behavior of the electrons and the localized character of the blue emission in β-Ga_2O_3. This model suggests that defects are inhomogeneously spread in β-Ga_2O_3 forming shallow donor clusters responsible for the degenerate semiconductor properties. Minority acceptors are located between the clusters and the blue emission occurs at acceptor sites after tunnel capture of an electron from a donor cluster by a hole on an acceptor.

2. EXPERIMENTAL

Single crystals of β-Ga_2O_3 were grown by the Verneuil method from commercial 4N grade gallium oxide powder. Some crystals were intentionally doped with 800 to 500 ppm mass of ZrO_2, since Zr^{4+} is known to enhance both conductivity and blue luminescence in gallium oxide [4, 8]. Spectrochemical analysis showed that the residual Zr content in the doped crystals lies in the range 200–650 ppm. The other majority impurities are Ca (50–400 ppm) and Fe (50–500 ppm). All the crystals were light blue, indicating the presence of free electrons [4]. Four point DC conductivity measurements were performed on needle-shaped single crystals along the crystallographic *b* direction, with indium contacts. ESR spectra were recorded with an X-band (9.4 GHz) ESP300e Bruker spectrometer equipped with a TE_{102} cavity and an ESR9 helium flow cryostat from Oxford Instruments. The luminescence spectra were obtained under UV excitation at 266 nm (4.67 eV) with the fourth harmonic of a Nd:YAG laser from BMI. The emission was detected by a HR250 monochromator from Jobin-Yvon equipped with a 300 groove/mm grating blazed at 500 nm. An optical multichannel analyzer allowed spectra acquisition, either in continuous or in time-resolved modes. The low temperature spectra were obtained with a helium gas flow cryostat from CTI Cryogenics. They were recorded under dynamic increase of temperature from 12 to 300 K at an approximate rate of 100 K/h. For luminescence spectra above room temperature, the sample was set in a sample holder at the top of a copper shaft projecting into a tubular furnace. The temperature was measured in the sample holder, close to the sample. High temperature spectra were recorded under dynamic decrease of temperature from 500 to 300 K at the rate of 100 K/h. Excitation spectra were obtained under excitation from a 300 W xenon lamp and selected with a Jobin-Yvon H25 monochromator with a 1200 groove/mm grating blazed at 285 nm. The emission was detected with a Jobin-Yvon HR1000 monochromator equiped with a 1200 groove/mm grating blazed at 500 nm and a R928 Haramatsu photomultiplier.

3. RESULTS

3.1. *Low temperature ESR and conductivity*

Fig. 1(a) shows an example of temperature dependence of the DC conductivity along the *b* axis for an as-grown single crystal of β-Ga_2O_3. The conductivity is slightly thermally activated between 50 and 150 K due to the thermal excitation of the electrons from the donor states to the conduction band. The conductivity decreases only by a factor of 1.5 when the temperature varies from 300 to 4 K, so that a strong conductivity below 50 K, slightly decreasing when temperature increases, is still observed. This is the first evidence of free electrons in donor states. The second evidence is the existence of a motionally narrowed ESR signal in the whole temperature range (insets in Fig. 1(a)) and especially below 50 K, with a very small linewidth $\Delta B \approx 0.2$ mT at 20 K. Previous measurements of the electron spin–lattice relaxation time T_1 versus temperature [12], shown in Fig. 1(a) for memory, indicate a behavior of the electron spin relaxation similar to that of conductivity. This shows that electron spins relax via the Elliott mechanism typical of free electrons [19]. According to this mechanism, spin–lattice T_1 and spin–spin T_2 relaxation times are equal and related to the correlation time of

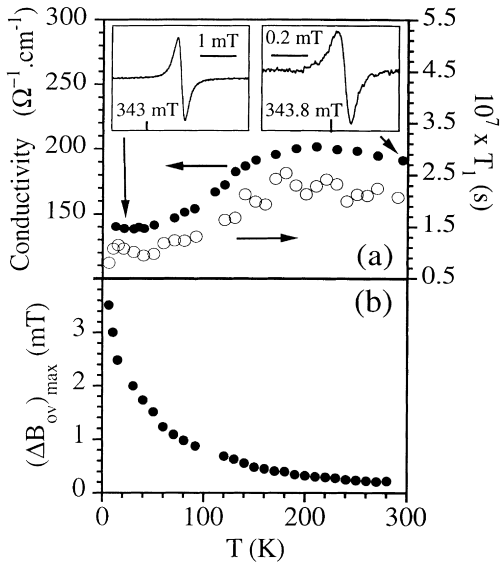

Fig. 1. (a) DC conductivity (●) along the *b* axis for a β-Ga_2O_3 single crystal and spin–lattice electron relaxation time T_1 (○). Insets: motionally narrowed ESR signals at room temperature and at $T = 20$ K for a single crystal of β-Ga_2O_3. Microwave frequency, 9.44614 GHz (20 K) and 9.43723 GHz (room temperature); microwave field, 7×10^{-3} mT (20 K) and 2.10^{-3} mT (room temperature). (b) Magnetic field $(\Delta B_{ov})_{max}$ induced by dynamic polarization of gallium nuclear spins by saturation of the conduction electron spin resonance.

conductivity τ_c by:

$$T_1 \approx T_2 \propto \frac{\tau_c}{(\Delta g)^2} \qquad (1)$$

where Δg is the *g*-factor deviation from the free electron *g* value, $g_e = 2.0023$. In β-Ga_2O_3, the *g*-factor is anisotropic and slightly sample dependent. Typical principal *g* values are $g_x = 1.9601 \pm 5 \times 10^{-4}$, $g_y = 1.9629 \pm 5 \times 10^{-4}$ and $g_z = 1.9649 \pm 5 \times 10^{-4}$ with the principal *z*-axis parallel to *b* and the principal *y*-axis making an angle with *a* (*y*,*a*) = 30°. The small deviation from the free electron *g* value is related to spin–orbit coupling due to a slight contribution of 4*p* orbitals from gallium to the bottom of the conduction band.

Consequently this indicates that, in the whole temperature range, spins detected by ESR actually correspond to conduction electrons. The final evidence for delocalized electrons in donor states is a strong dynamic nuclear polarization. This phenomenon, known as the Overhauser effect [20], arises when electrons are delocalized over a great number of non-zero nuclear spins, which in β-Ga_2O_3 are those of the two gallium isotopes ^{69}Ga and ^{71}Ga, both with $I = 3/2$. In that case the hyperfine interaction is motionally averaged and the saturation of the ESR transition creates a strong nuclear magnetic field, $(\Delta B_{ov})_{max}$, causing a shift of the ESR signal at high microwave power [12]. The nuclear field $(\Delta B_{ov})_{max}$ for a single crystal is plotted in Fig. 1(b) as a function of temperature *T*. The sharp increase of $(\Delta B_{ov})_{max}$ as *T* approaches zero is related to the contribution of the thermal nuclear polarization which obeys a Curie-type law [12]. Nevertheless, the dynamic nuclear polarization is still significant in the temperature range $T < 50$ K, where conduction electrons lie in the donor states. Thus the delocalized properties of the electrons in donor states show that the Mott criterion for impurity band conduction is achieved in β-Ga_2O_3:

$$N_d^{1/3} \times R_d > 0.26 \qquad (2)$$

where N_d is the donor concentration and R_d the donor Bohr radius, so that donor wave functions merge into a donor band extending over a wide range in the solid. The observation of an electron conduction and of a motionally narrowed ESR signal in the temperature range $T < 50$ K where electrons are in the donor band indicates that this band is only partially filled. This is in favor of the existence of minority acceptor defects, already proposed by several authors [8, 16], which can trap a few electrons from the donor band so that the Fermi level lies inside this band.

3.2. *Absorption, emission and excitation spectra of the blue luminescence*

Our samples contain free electrons at very low temperatures, a phenomenon which has not been reported in earlier work on the luminescence properties of ESR silent gallium oxide [7]. The question then arises as to whether our samples also present the same optical properties as the samples studied in the literature. Fig. 2 shows the broad emission of an undoped single crystal at room temperature upon excitation at 4.67 eV (266 nm), an energy smaller than the band gap (4.9 eV). This spectrum peaks at about 2.85 eV in the blue range. At room temperature, this luminescence can be excited in three overlapping bands indicated by arrows in Fig. 2. The first two bands correspond to the two low energy shoulders in the absorption spectrum while the shoulder at higher

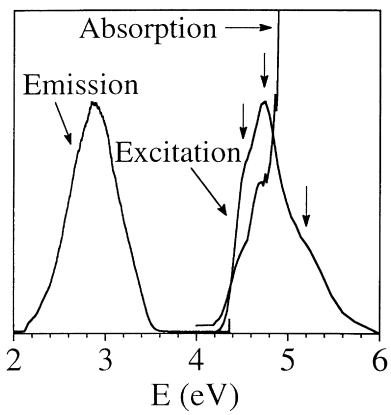

Fig. 2. Luminescence spectrum of an as-grown undoped single crystal under excitation at 4.67 eV and excitation spectrum of the blue emission, observed at 2.95 eV. Also shown is the absorption spectrum. All the spectra were recorded at room temperature.

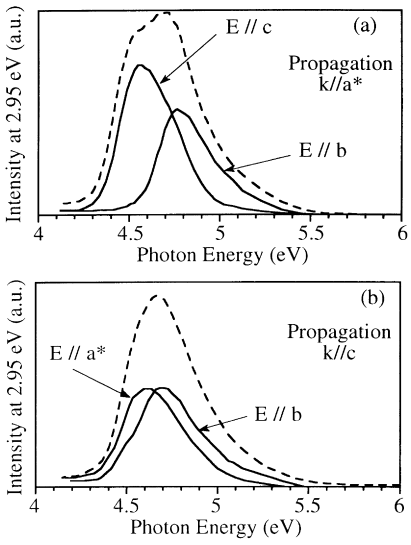

Fig. 3. Room temperature excitation spectra under polarized light (——) and unpolarized light (- - -) of the blue luminescence at 2.95 eV for an as-grown single crystal. (a) Light propagation perpendicular to the (100) plane. (b) Light propagation along the *c* axis.

energy coincides with the strong band-to-band intrinsic absorption (Fig. 2). An important Stokes shift of about 1.7 eV can be noticed, which indicates a strong electron–phonon coupling and means that the recombining charges are strongly localized. The excitation under polarized light and with propagation vector $\boldsymbol{k}//\boldsymbol{a}^*$ (Fig. 3(a)) and $\boldsymbol{k}//\boldsymbol{c}$ (Fig. 3(b)) shows that the lower energy excitation band peaks at about 4.56–4.6 eV and corresponds to an absorption with electric field $\boldsymbol{E}\perp\boldsymbol{b}$. The second excitation band peaks at 4.7–4.76 eV and corresponds to an absorption with $\boldsymbol{E}//\boldsymbol{b}$. The emission spectrum under UV excitation as well as the excitation spectra either under polarized or unpolarized light are in full agreement with earlier results [6–8]. Fig. 4 compares the emission spectra at room temperature and at 12 K upon excitation at 4.67 eV for a Zr-doped crystal. The straight edges on these spectra at 2.1 eV are due to the insensitivity of the detecting diodes below this energy. At room temperature and besides the blue emission, the UV emission can be also excited, resulting in a shoulder in the spectrum at about 3.2 eV. On the contrary at $T = 12$ K, only the blue emission occurs upon 4.67 eV excitation (Fig. 4). This observation is also in agreement with the results of a previous study in which it was observed that at 5 K the blue emission could only be excited with energies slightly below the band gap [8]. This confirms the attribution of the blue luminescence to the excitation of acceptor defects close to the valence band.

3.3. *Decay of the blue luminescence*

Fig. 5 shows the emission spectra at room temperature of an undoped blue single crystal at different delays after the exciting 4.67 eV laser pulse. For short delays after excitation ($t \leq 1$ μs) a fast decaying UV component can be observed on the spectra which adds to the blue emission. This UV component vanishes for $t > 1$ μs, so that only the blue emission remains. This fast decay for the UV emission is consistent with earlier observations where a characteristic decay time was found of the order of 30 ns [6]. Fig. 6 shows a plot of the total emitted intensity (calculated by integration of the spectra) at time *t* after the pulse for two samples, the first corresponding to spectra of Fig. 5, the second to a single crystal doped with Zr^{4+}. For $t \leq 1$ μs, the decay of the whole emission spectrum is mainly driven by the fast decay of the UV contribution but for $t > 1$ μs, the decay is characteristic of the blue emission only. It can be observed that the time dependence of the blue luminescence is the same for the two samples and is nearly independent of temperature. Previous observations on the decay of the blue luminescence are contradictory. Blasse and Bril observed a fast decay similar to that of the UV emission [6] while Harwig and Kellendonk observed a rather long decay with a

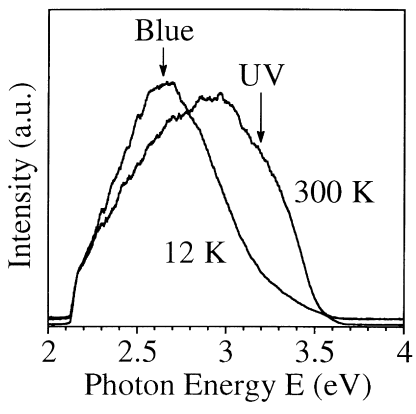

Fig. 4. Luminescence spectra of a Zr-doped single crystal at room temperature and 12 K under excitation at 4.67 eV, in the acceptor absorption band.

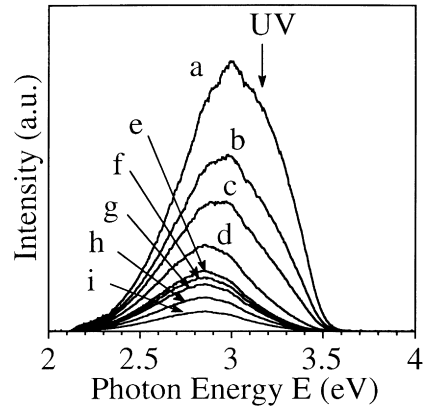

Fig. 5. Time evolution of luminescence spectrum of an as-grown single crystal at room temperature after a laser pulse at 4.67 eV: (a) $t = 0.5$ μs; (b) $t = 0.75$ μs; (c) $t = 1$ μs; (d) $t = 2$ μs; (e) $t = 5$ μs; (f) $t = 7$ μs; (g) $t = 10$ μs; (h) $t = 20$ μs; (i) $t = 50$ μs.

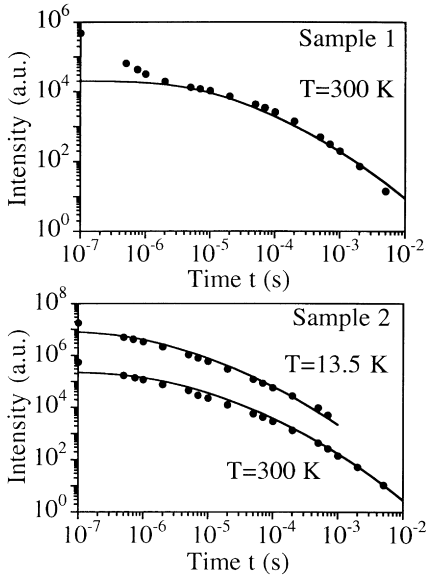

Fig. 6. Decay of the luminescence intensity for two single crystals. (top) Same samples as in Fig. 5 (as-grown single crystal). (bottom) Zr-doped single crystal. The solid lines represent the theoretical evolution corresponding to eqn (10), with the following parameters: (top) $N = 8 \times 10^{17}$ cm^{-3}, $W_{max} = 10^6$ s^{-1}; (bottom) $N = 10^{18}$ cm^{-3}, $W_{max} = 10^7$ s^{-1} ($T = 13.5$ K) and $W_{max} = 5 \times 10^6$ s^{-1} ($T = 300$ K).

characteristic time of about 120 μs [8]. In our case, the blue luminescence could be detected up to a few milliseconds, which is more consistent with the results of Harwig and Kellendonk [8]. The kinetics is neither exponential—which means that it is not driven by the transition probability of the recombination center—nor hyperbolic, contrary to the observations of Harwig and Kellendonk [8].

3.4. *Temperature dependence of the blue luminescence upon sub-band gap excitation*

The effect of temperature on the luminescence of β-Ga_2O_3 has already been studied in the case of excitation through the gap in the intrinsic absorption band [7, 8, 14]. In that case, only the UV emission is observed at low temperature. When the temperature is raised to 300 K, the intensity of the UV emission decreases and simultaneously the blue emission emerges. The blue emission is then totally quenched above 400 K.

In the present work, the samples were excited at 4.67 eV in the specific absorption band of the acceptor defects, below the intrinsic absorption, and a different behavior for the temperature dependence of the blue emission was observed. Fig. 7 shows the luminescence spectra of a Zr-doped single crystal between 13.5 and 280 K. These spectra were recorded in time-resolved mode with acquisition immediately after the exciting laser pulse. A long intensification of 1 ms of the detecting diodes privileges the long decaying components of the emission spectrum and therefore was used to record

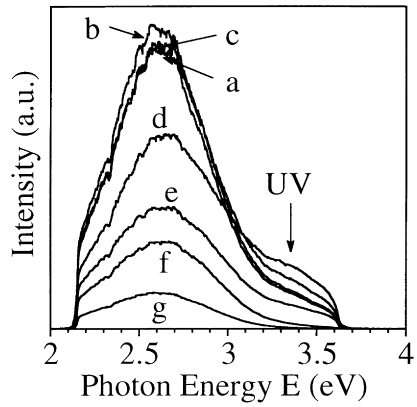

Fig. 7. Temperature dependence of luminescence spectra for a Zr-doped single crystal below room temperature: (a) $T = 13.5$ K; (b) $T = 50$ K; (c) $T = 100$ K; (d) $T = 150$ K; (e) $T = 200$ K; (f) $T = 240$ K; (g) $T = 280$ K. It can be noticed there is a burst of UV emission (3.34 eV) around 150 K.

specifically the blue emission. As seen before, at low temperature and upon excitation at 4.67 eV, only the blue emission occurs. The full circles in Fig. 8(a) represent the intensity at the emission maximum (2.64 eV). When the temperature is raised from 13.5 to 280 K, the intensity of the blue emission decreases. In the temperature range 300–500 K, another quenching region is observed for the blue emission (Fig. 8(b)). The intensity of the blue emission at 2.64 eV versus temperature follows the usual law for thermal quenching [21]:

$$I(T) = \frac{I_0}{1 + A\exp(-\Delta E/kT)} \tag{3}$$

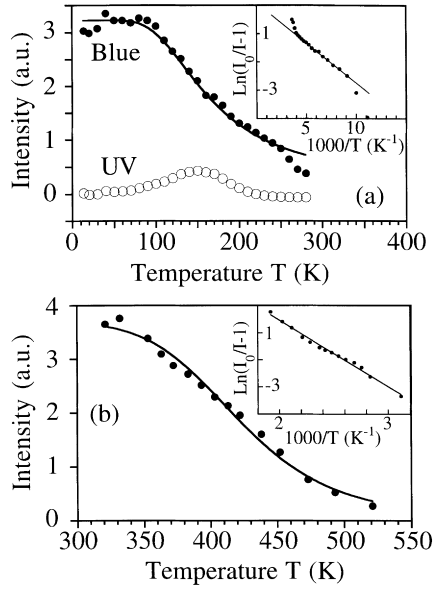

Fig. 8. Temperature dependence of the emission intensity at 2.64 eV (●) and 3.34 eV (○). Solid lines correspond to the theoretical variation according to eqn (3) with parameters $\Delta E = 0.05$ eV, $A = 28$ (top figure) and $\Delta E = 0.42$ eV, $A = 1.1 \times 10^5$ (bottom figure). The inset shows the plot of $\ln[I_0/I(T) - 1]$ versus $1/T$. The slopes of the linear domains give the activation energies ΔE.

The plot of $\ln [I_0/I(T) - 1]$ versus $1/T$ shows two linear domains, the first one in the temperature range 50–250 K (inset in Fig. 8(a)) corresponding to an activation energy $\Delta E_1 \approx 0.05$ eV, the second one in the range 300–500 K (inset in Fig. 8(b)) corresponding to a second activation energy $\Delta E_2 \approx 0.42$ eV. Along with the decrease of the blue emission upon temperature increase in the range 13.5–280 K, an enhancement of the UV luminescence is observed, with a shoulder rising in the UV domain (about 3.34 eV) in the spectra of Fig. 7. The intensity of the UV emission at 3.34 eV is plotted in Fig. 8(a) after subtraction of a background contribution following eqn (3) due to the wings of the broad blue emission. One can observe that the enhancement of the UV emission has a maximum at $T \approx 150$ K. Therefore, the behavior of both the blue and UV emissions upon specific excitation of the acceptor defects at 4.67 eV is exactly opposite to what is observed with excitation through the gap [7, 8, 14].

4. DISCUSSION

The correlation between the blue luminescence and the electronic conductivity [8] indicates that oxygen vacancies, responsible for the *n*-type conductivity, are also involved in the blue emission process. Moreover, the excitation of the blue luminescence with photon energy slightly below the band gap [8], and confirmed in the present work, shows that acceptor defects with ground state close to the valence band also participate in the blue emission. Harwig and Kellendonk then suggested that these defects should contain gallium vacancies, since doping with Si or Zr which increases the concentration in gallium vacancies, also enhances the blue luminescence [8]. These vacancies are naturally present in undoped blue luminescent crystals elaborated from melt, due to the volatilization of Ga_2O. According to Vasil'tsiv *et al.*, the acceptors would be formed by a gallium–oxygen vacancy pair [16], denoted $(V_O, V_{Ga})'$ in the Kröger–Vink notation. We believe this type of defect to be more likely than a single heavily charged gallium vacancy V_{Ga}'''. On the basis of the above observations, Harwig and Kellendonk suggested that the blue emission would originate from the recombination of an electron on a donor and a hole on an acceptor [8]. Our investigation of the temperature dependence of the blue emission upon specific excitation of the acceptor defects agrees with this hypothesis. After excitation of the acceptor, a hole on the acceptor and an electron on a donor are created according to the following formal equation:

$$(V_O, V_{Ga})' + V_O^{\cdot} + h\nu \rightarrow (V_O, V_{Ga})^X + V_O^X \qquad (4)$$

and the blue emission occurs via the reverse reaction. Therefore, with increasing temperature, the blue emission can be quenched either by electron detrapping

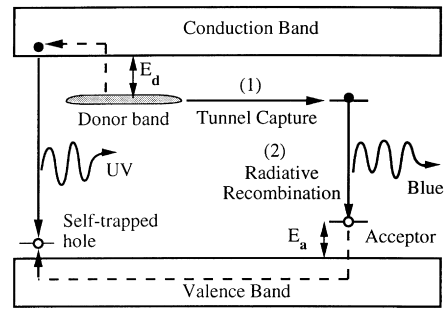

Fig. 9. Model for the blue luminescence in gallium oxide. An electron in a donor cluster forming a donor band is captured via a tunnel transfer (channel 1) by a hole on an acceptor to form a trapped exciton, which recombines radiatively (channel 2) emitting a blue photon. When the temperature is raised, electrons on donors and holes on acceptors can be thermally detrapped (- - -). They migrate through the solid and recombine via a self-trapped exciton, with emission of a UV photon.

from a donor to the conduction band according to:

$$V_O^X \rightarrow V_O^{\cdot} + e_{cb}^- \qquad (5)$$

or by hole detrapping from an acceptor to the valence band according to:

$$(V_O, V_{Ga})^X \rightarrow (V_O, V_{Ga})' + h_{vb}^{\cdot} \qquad (6)$$

These processes are shown by dotted lines in Fig. 9. The activation energies of each process should then correspond to the defect ionization energies. The first region of quenching with activation energy $\Delta E_1 \approx 0.05$ eV close to the donor ionization energy $E_d \approx 0.04$ eV corresponds to the electron detrapping while the second region with activation energy $\Delta E_2 \approx 0.42$ eV could correspond to the hole detrapping. We thus obtain the acceptor ionization energy:

$$E_a = \Delta E_2 \approx 0.42 \text{ eV} \qquad (7)$$

The enhancement of the UV luminescence at 150 K can also be explained by this model. When both electron and hole are detrapped, they can migrate through the solid and meet to form a self-trapped exciton which recombines and emits a UV photon (Fig. 9). Therefore, the UV enhancement appears as a thermally stimulated luminescence. The temperature at the maximum of UV luminescence is mainly determined by the deepest trap, here the acceptor which is a hole trap. Thus, from the Urbach law [22], we can derive a rough estimate of the trap depth, i.e. the acceptor ionization energy:

$$E_a \approx \frac{T_m}{500} \text{ (eV)} \qquad (8)$$

where $T_m \approx 150$ K is the temperature at the maximum of UV luminescence. Therefore, we obtain a value $E_a \approx 0.3$ eV. Due to the approximative validity of eqn (8) in our case, this value can be considered to be in acceptable agreement with the value $E_a \approx 0.42$ eV determined previously from the thermal quenching of the blue emission.

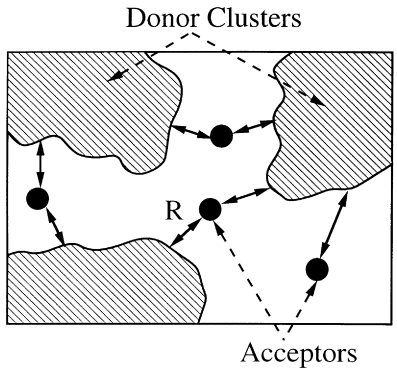

Fig. 10. Cluster model for the donors (oxygen vacancies) in gallium oxide. Oxygen vacancies are gathered in shallow clusters to form an impurity band responsible for the delocalized properties of electrons (conductivity and magnetic properties). Acceptors, responsible for the localized blue luminescence, are located between donor clusters at some random distance R from the clusters.

However, the existence of a donor band evidenced by the conductivity below 50 K and the motionally narrowed CESR signal, and the delocalized behavior of electrons in donor states, seem at first sight to be opposed to the localized character of the blue emission shown by the strong Stokes shift. We suggest here a model which can solve this apparent contradiction. The formation of an acceptor requires the association of an oxygen vacancy with a gallium vacancy to form a pair $(V_O, V_{Ga})'$ so that, in the vicinity of acceptors, the solid must be deprived of donors and the impurity band must be interrupted. Therefore, it can be imagined that donors are assembled in shallow clusters with between some minority acceptors at some distance R from the cluster boundaries (Fig. 10). According to this model, the donor clusters with delocalized electron states would be responsible for the conduction and the bistable magnetic properties, while the blue emission would result from a two-step recombination process between an electron in a donor cluster and a hole on an acceptor (Fig. 9). The first step consists of a tunnel transfer of an electron from a donor cluster to a neutral acceptor to form a trapped exciton. The second step is a radiative recombination of the exciton at the acceptor site, which explains the localized character of the blue luminescence. Since the decay is not exponential, the rate determining step for the blue emission must be the tunnel capture of an electron by an acceptor. This situation is similar to the donor–acceptor pair (DAP) model of Thomas *et al*. [23] and we shall now see that the kinetic law for DAP recombination can be adapted to our cluster model. In the DAP model, minority defects, in our case the acceptors, are assumed to be surrounded by a random distribution of majority defects, in our case the donors, at distance R from an acceptor. Before emission, all donors and acceptors are assumed to be neutral. By tunnel recombination of an electron at a donor site with a hole at an acceptor site, a photon is emitted with energy given by:

$$h\nu = E_g - (E_d + E_a) + \frac{e^2}{4\pi\varepsilon R} \pm nE_{phonon} \qquad (9)$$

where E_g is the band gap, E_d and E_a the donor and acceptor ionization energies, respectively and E_{phonon} the energy of phonons involved in the radiative transition, with $n = 0, 1, 2\ldots$ The term $E_c = e^2/4\pi\varepsilon R$ corresponds to the coulombic interaction between ionized donor and acceptor. In the DAP model, the total intensity emitted at time t after excitation is given by [23]:

$$I(t) = \left\{ 4\pi N \int_0^\infty W(R)\exp\left[-W(R)t\right]R^2\,\mathrm{d}R \right\} \times \exp\left[4\pi N \int_0^\infty \left\{\exp\left[-W(R)t\right] - 1\right\}R^2\,\mathrm{d}R \right] \qquad (10)$$

where N is the majority defect concentration, R is the distance between a donor and an acceptor and $W(R)$ the recombination probability for a donor–acceptor pair with separation R. The following expression for $W(R)$ was calculated [23]:

$$W(r) = W_{max}\exp(-2R/R_d) \qquad (11)$$

where R_d is the Bohr radius of the shallowest defect. Strictly speaking, eqn (11) holds when one defect is much shallower than the other. In the case of defects in β-Ga_2O_3, donors are actually shallower than acceptors since $E_d \approx 0.04$ eV $\ll E_a \approx 0.4$ eV. Eqn (11) also assumes that the shallowest state can be described by an s-type wave function and means that the recombination probability is merely proportional to the electron density created by a donor at an acceptor site. However, in our model, the donors must be considered as gathered in clusters to account for the delocalized properties of the donor states at low temperature. Between these clusters, the space is occupied by acceptors. Therefore, eqn (10) can also be applied to our situation, if we consider that the distance R represents the distance between an acceptor and the boundary of a donor domain (Fig. 10). Also, although the donor wave function is delocalized over the donor domains, the contribution to the electron density at acceptor sites mainly arises from boundary states of the donor domains, which should have an exponential decay similar to that of a hydrogen-like wave function. Thus, we believe that eqn (11) for the recombination probability is also valid in our case, to a good approximation. For donors in Ga_2O_3, the Bohr radius is $R_d \approx 18$ Å [12]. Therefore, the simulation of the blue emission decay with eqn (10) contains only two adjustable parameters: the donor concentration $N = N_d$ and the maximum recombination probability W_{max}. The agreement between eqn (10) and the experimental data is rather good with $N = N_d \approx 10^{18}$ cm^{-3} and $W_{max} \approx 10^6 - 10^7$ s^{-1} (Fig. 6). The value

for N is fully consistent with donor concentrations measured in our Ga_2O_3 samples and the value for W_{max} lies in the range of values measured with other compounds exhibiting a donor–acceptor-like luminescence [24]. Therefore we can conclude that the rate determining step for the blue luminescence in non-stoechiometric gallium oxide is a tunnel capture of an electron from conducting donor clusters by a hole on an acceptor at some distance from the clusters to form a rapidly recombining exciton trapped on the acceptor.

However, the donor–acceptor-type model used to explain the blue luminescence decay in Ga_2O_3 should involve two effects, characteristic of DAP recombination, that are not observed in the present case. The first effect is a shift with time of the maximum of emission towards lower energies (t-shift). This shift is due to the fact that close donor–acceptor pairs recombine with higher energy and faster than more distant pairs, which also emit at lower energy. The photon energy $h\nu_{max}(t)$ at the maximum of emission at time t was calculated [25] for a zero-phonon transition, when donors are shallower than acceptors, and is given by:

$$\ln(W_{max}t) = 4\frac{E_d}{E_{c,max}(t)} + \ln\left[1 - \frac{E_{c,max}(t)}{E_d}\right] \qquad (12)$$

where $E_{c,max}(t)$ is defined from eqn (9) with $n = 0$ by

$$E_{c,max}(t) = h\nu_{max}(t) - E_g + E_d + E_a \qquad (13)$$

Since eqn (12) requires $E_{c,max}(t) < E_d$, it can be deduced from eqn (13) that the shift of the maximum of emission $h\nu_{max}(t)$ cannot exceed the ionization energy of the shallowest defect E_d. In the case of gallium oxide, the donor ionization energy is $E_d \approx 0.04$ eV and such a small shift cannot be observed, because of the broadness of the emission spectrum ($\approx$ 0,6 eV at half-height). The second predicted effect is that the luminescence decay should be speeded up when the temperature is raised since electrons on donors far from an acceptor and with low recombination probability can be thermally detrapped and trapped again on closer donors with higher recombination probability. In the case of gallium oxide, the decay kinetics is independent of temperature (Fig. 6). This is consistent with our cluster model for the donors, since electrons are delocalized in donor states so that they can always come as close as possible to an acceptor, whatever the temperature.

5. CONCLUSION

Electrons in donor states of β-Ga_2O_3 can exhibit paradoxically both delocalized properties—i.e. conductivity, motionally narrowed ESR lines and dynamic nuclear polarization by the Overhauser effect [12]—and localized properties such as a broad blue luminescence with a strong Stokes shift [6, 8]. We showed that this duality is related to a particular defect microstructure. Donors (oxygen vacancies) are assembled in clusters with delocalized electron states responsible for low temperature conductivity, motionally narrowed ESR and dynamic nuclear polarization, while acceptors (pairs of oxygen and gallium vacancies) are located between at some distance from the cluster boundaries. The investigation of the temperature dependence of the blue luminescence in gallium oxide, upon specific excitation of the acceptor defects, confirmed earlier suggestions in the literature that both donors and acceptors are involved in the blue emission process. A quantitative analysis of the blue emission decay allowed us to clarify the mechanism of this luminescence. We conclude that the blue emission results from a rate determining transfer by tunnel effect of an electron from a donor cluster to a hole trapped at an acceptor site. Subsequently a fast electron–hole recombination occurs at the acceptor site with strong electron–phonon coupling giving rise to the blue emission.

Acknowledgements—The authors are indebted to M. Patrick Aschehoug for technical assistance in fluorescence experiments.

REFERENCES

1. Tippins, H. H., *Phys. Rev.*, 1965, **140**, A316.
2. Lorenz, M. R., Woods, J. F. and Gambino, R. J., *J. Phys. Chem. Solids*, 1967, **28**, 403.
3. Harwig, T., Wubs, G. J. and Dirksen, G. J., *Solid State Commun.*, 1976, **18**, 1223.
4. Harwig, T. and Schoonman, J., *J. Solid State Chem.*, 1978, **23**, 205.
5. Herbert, W. C., Minnier, H. B. and Brown, J. J. Jr., *J. Electrochem. Soc.*, 1969, **116**, 1019.
6. Blasse, G. and Bril, A., *J. Phys. Chem. Solids*, 1970, **31**, 707.
7. Harwig, T., Kellendonk, F. and Slappendel, S., *J. Phys. Chem. Solids*, 1978, **39**, 675.
8. Harwig, T. and Kellendonk, F., *J. Solid State Chem.*, 1978, **24**, 255.
9. Binet, L., Gourier, D. and Minot, C., *J. Solid State Chem.*, 1994, **113**, 420.
10. Dirksen, G. J., Hoffman, A. N. J. M., van de Bout, T. P., Laudy, M. P. G. and Blasse, G., *J. Mater. Chem.*, 1991, **1**, 1001.
11. Edwards, D. D., Mason, T. O., Goutenoir, F. and Poeppelmeier, K. R., *Appl. Phys. Lett.*, 1997, **70,** 1706; Ueda, N., Hosono, H., Waseda, R. and Kawazoe, H., *Appl. Phys. Lett.*, 1997, **70,** 3561; Ueda, N., Hosono, H., Waseda, R. and Kawazoe, H., *Appl. Phys. Lett.*, 1997, **71,** 933; Minami, T., Yamada, H., Kubota, Y. and Miyata, T., *Jpn. J. Appl. Phys.*, 1997, **36,** L1191; Phillips, J. M., Kwo, J., Thomas, G. A., Carter, S. A., Cava, R. J., Hou, S. Y., Krajewski, J. J., Marshall, J. H., Peck, W. F., Rapkine, D. H. and van Dover, R. B., *Appl. Phys. Lett.*, 1994, **65,** 115.
12. Aubay, E. and Gourier, D., *Phys. Rev. B*, 1993, **47**, 15023.
13. Binet, L. and Gourier, D., *J. Phys. Chem.*, 1996, **100**, 17630.
14. Vasil'tsiv, V. I. and Zakharko, Ya. M., *Sov. Phys. Solid State*, 1983, **25**, 72.
15. Kuznetsov, A. I., Abramov, V. N. and Uibo, T. V., *Opt. Spectrosc. (USSR)*, 1985, **58**, 368.
16. Vasil'tsiv, V. I., Zakharko, Ya. M. and Prim, Ya. I., *Ukr. Fiz. Zh.*, 1988, **33**, 1320.
17. Bozon-Verduraz, F., Potvin, C. and Pannetier, G., *J. Chim. Phys. (Fr)*, 1970, **67**, 1608.

18. Mott, N. F., *Proc. Phys. Soc. London*, 1949, **62**, 416.
19. Elliott, R. J., *Phys. Rev.*, 1954, **96**, 266.
20. Overhauser, A., *Phys. Rev.*, 1953, **92**, 411.
21. Dean, P. J., *Progress in Solid State Chemistry*, Vol. 8. Pergamon Press, Oxford, 1973, p. 64.
22. Urbach, F., *Wiener Ber.*, 1930, **139**, 363.
23. Thomas, D. G., Hopfield, J. J. and Augustyniak, W. M., *Phys. Rev.*, 1965, **140**, A202.
24. Dean, P. J., *Progress in Solid State Chemistry*, Vol. 8. Pergamon Press, Oxford, 1973, p. 49.
25. Colbow, K., *Phys. Rev.*, 1966, **141**, 742.